Dalton Transactions

Cite this: *Dalton Trans.*, 2012, **41**, 201

www.rsc.org/dalton

PAPER

On the electronic structure of nitro-substituted bipyridines and their platinum complexes†

Paul R. Murray,*[a] Stephen Crawford,[a] Alice Dawson,[a] Alexander Delf,[a] Calum Findlay,[a] Lorna Jack,[a] Eric J. L. McInnes,[b] Salma Al-Musharafi,[a] Gary S. Nichol,[a] Iain Oswald[a] and Lesley J. Yellowlees*[a]

Received 2nd August 2011, Accepted 29th September 2011
DOI: 10.1039/c1dt11456e

We report the preparation and electrochemical studies of a systematic series of mono- and di-nitro-substituted 2,2′-bipyridine (bipy) compounds [x-NO_2-bipy (x = 3,4) and x,x′-$(NO_2)_2$-bipy (x,x′ = 3, 4, 5)] and their complexes with platinum(II), [Pt(x-NO_2-bipy)Cl_2] and [Pt(x,x′-$(NO_2)_2$-bipy)Cl_2]. The effect of the number and substitution pattern of the nitro groups on the low-lying acceptor molecular orbitals (involved in charge transfer transitions) is probed by *in situ* UV/Vis/NIR and EPR spectroelectrochemical methods, supported by DFT calculations. The LUMOs of x-NO_2-bipy (x = 3–5) are largely localised on the NO_2-pyridyl moiety; this is also true of their {$PtCl_2$} complexes but with a small but significant shift of electron density from the nitro groups. The LUMOs of x,x′-$(NO_2)_2$-bipy with x = 3 and 5 are delocalised over both NO_2-pyridyl rings, but for 4,4′-$(NO_2)_2$-bipy is localised on a single NO_2-pyridyl ring. In all cases the LUMO of the [Pt(x,x′-$(NO_2)_2$-bipy)Cl_2] complexes is delocalised over both nitro-pyridyl rings. For all complexes, the 4(4′) derivatives allows greatest overlap with metal valence orbitals in the LUMO.

Introduction

Reported applications for charge transfer complexes of 2,2′-bipyridine (bipy) include chemodosimetry,[1] hydrogen production by artificial photosynthesis,[2,3] and dye sensitised solar cells.[4–9] We have been probing the electronic structure, and the nature of the important charge transfer excited states, in such species by electrochemical techniques coupled with UV/Vis and EPR spectroscopies, focusing in particular on the family of square planar platinum(II) complexes.[10–12] Recently, we have investigated the effects of strongly electron withdrawing groups on the bipyridyl, for example, in 4-NO_2-bipy.[13] We showed that the LUMOs of 4-NO_2-bipy and its [Pt(4-NO_2-bipy)Cl_2] complex, are largely localised on the nitro-bearing half of the bipyridyl group. Moreover, for the complex there is significantly less admixture of Pt valence orbitals to the LUMO compared to the [Pt(bipy)Cl_2] parent complex. Previously, we have shown that [Pt(4,4′-$(NO_2)_2$-bipy)Cl_2] has a low-lying near degenerate pair of LUMOs delocalised over both rings.[14] Since such effects could have significant effects on relaxation mechanisms of the charge transfer excited states, we now extend this study to other nitro-bearing bipyridyls. In particular, we prepare a systematic series of 3–5 mono- and 3,3′–5,5′ di-substituted nitro-bipyridyls and their Pt(II) complexes, and probe their electronic character using combined spectroscopic and electrochemical techniques. Although there are a number of reports of transition metal complexes of 4-NO_2-bipy and 4,4′-NO_2-bipy ligands,[15–27] as these isomers are easiest to prepare, there are few reports with 3, 3′, 5 and 5′ nitro-bipyridyls.[28–30]

Results and discussion

Synthesis

All ligands were synthesised either according to literature methods or modifications thereof. Platinum(II) complexes [Pt(L)Cl_2] (L = nitro-derivatised bipy) were prepared simply and in good yield by reflux with $K_2[PtCl_4]$ in water.

Crystal structures

Crystal structures were obtained for the 5,5′-$(NO_2)_2$-bipy and 3-NO_2-bipy free ligands, and for the complex [Pt(3,3′-$(NO_2)_2$-bipy)Cl_2] (see Experimental). The structures of 5,5′-$(NO_2)_2$-bipy and 3-NO_2-bipy (Figures S1 and S2, ESI†) hold few surprises, with the pyridyl rings lying *trans* with respect to each other (for 5,5′-$(NO_2)_2$-bipy this is a consequence of crystallographic inversion symmetry), and with similar metric parameters to those reported

---

[a] *EaStCHEM, School of Chemistry, University of Edinburgh, King's Buildings, West Mains Road, Edinburgh, UK. E-mail: p.r.murray@ed.ac.uk, l.j.yellowlees@ed.ac.uk; Fax: +44-(0)131-650-6453; Tel: +44-(0)131-650-4759*

[b] *The EPSRC UK National Electron Paramagnetic Resonance Service at The University of Manchester, School of Chemistry, Manchester, M13 9PL, UK. E-mail: eric.mcinnes@manchester.ac.uk; Fax: +44(0)161-2755-6106; Tel: +44-(0)161-275-4669*

† Electronic supplementary information (ESI) available: Structures of 5,5′-$(NO_2)_2$-bpy and 3-NO_2-bpy; solvent dependence of redox potentials for 5,5′-$(NO_2)_2$-bpy and its {$PtCl_2$} complex; UV/Vis/NIR data. CCDC reference numbers 660844 [5,5′-$(NO_2)_2$-bpy], 838414 and 838415. For ESI and crystallographic data in CIF or other electronic format see DOI: 10.1039/c1dt11456e

for 3,3′- and 4,4′-nitro-substituted derivatives.[31,32] 5,5′-$(NO_2)_2$-bipy is planar, while in 3-NO_2-bipy the two pyridyl rings are twisted with a torsion angle of 28.8°, much smaller than in 3,3′-$(NO_2)_2$-bipy (48.9°),[32] reflecting the presence of a single NO_2 group. Dark red crystals of [Pt(3,3′-$(NO_2)_2$-bipy)Cl_2] were grown by diffusion of diethyl ether into a *N*,*N*′-dimethylformamide (DMF) solution. The steric demands of the 3,3′-substituents force a significant twisting of the two pyridyl rings (Fig. 1). Although the torsion angle of 17.28(4)° is smaller than reported for other [Pt(3,3′-X_2-bipy)Cl_2] derivatives (25.5, 26.5 and 30.0° for X = CO_2Me,[33] CO_2H,[34] and CH_2OH,[34] respectively), the two nitro groups are forced to lie coplanar with shortest inter-nitro group N…O distances of 2.65 Å.

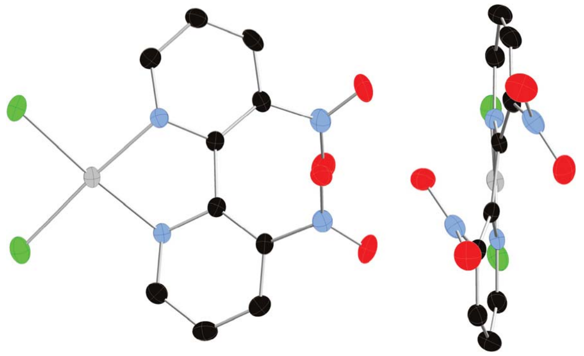

Fig. 1 Molecular structure of [Pt(3,3′-$(NO_2)_2$-bipy)Cl_2] viewed perpendicular to the {$PtCl_2$} plane (left) and bisecting the Cl–Pt–Cl angle (right) highlighting the steric clash of the two nitro groups. Scheme: Pt(grey), Cl (green), N (blue) and O (red); H omitted for clarity.

Electrochemistry

Cyclic voltammetry (CV) of the ligands in 0.1 M [$^nBu_4N$][BF_4] DMF solution reveals one or more one-electron reduction processes in each case [Table 1, including data for x-NO_2-pyridines (py) for comparison].

x-NO_2-bipy and x,x′-$(NO_2)_2$-bipy: The mono-substituted x-NO_2-bipy free-ligands undergo reduction at potentials which are a huge 1.1–1.4 V less negative than for bipy itself. These redox potentials are very similar to those observed for x-NO_2-py, which implies that the LUMO of x-NO_2-py is not significantly perturbed by substitution with a second py group. Surprisingly, addition of a second nitro group in x,x′-$(NO_2)_2$-bipy induces a further shift to more postive potentials of only 0.1–0.2 V.

Table 1 Reduction potentials[a] from cyclic voltammetry in 0.1 M [$^nBu_4N$][BF_4] DMF solution

Compound	E_1/V	E_2/V	$E_1 - E_2$/V
3-NO_2-py	−0.94	—	—
4-NO_2-py[13]	−0.74	—	—
bipy	−2.05[b]	—	—
3-NO_2-bipy	−0.98	−1.88[b]	—
4-NO_2-bipy[13]	−0.72	−1.74[b]	—
5-NO_2-bipy	−0.84	−1.63[b]	—
3,3′-$(NO_2)_2$-bipy	−0.79	−1.10	0.31
4,4′-$(NO_2)_2$-bipy	−0.64	−0.79	0.15
5,5′-$(NO_2)_2$-bipy	−0.61	−0.70	0.09
[Pt(bipy)Cl_2][12]	−1.06	−1.79	0.73
[Pt(3-NO_2-bipy)Cl_2]	−0.44	−0.88	0.44
[Pt(4-NO_2-bipy)Cl_2][13]	−0.34	−0.96	0.62
[Pt(5-NO_2-bipy)Cl_2]	−0.40	−0.94	0.54
[Pt(3,3′-$(NO_2)_2$-bipy)Cl_2]	0.01	−0.40	0.39
[Pt(4,4′-$(NO_2)_2$-bipy)Cl_2][14]	−0.26	−0.45	0.19
[Pt(5,5′-$(NO_2)_2$-bipy)Cl_2]	−0.18	−0.32	0.14

[a] Potentials *vs.* Ag/AgCl; [b] irreversible process, cathodic peak quoted.

[Pt(x-NO_2-bipy)Cl_2] and [Pt(x,x′-$(NO_2)_2$-bipy)Cl_2]: In all cases coordination to the {$PtCl_2$} fragment shifts $E_{\frac{1}{2}}$ to much less negative values. For all complexes except [Pt(3,3′-$(NO_2)_2$-bipy)Cl_2], the shift is 0.4–0.5 V compared to the free ligand, with the values for the di-substituted complexes being 0.1–0.2 V more positive than the mono-substituted equivalents (mirroring the free ligand behaviour). The outlier is [Pt(3,3′-$(NO_2)_2$-bipy)Cl_2] for which the first reduction potential is remarkably positive at +0.01 V. This is despite the fact that the free ligand is the hardest to reduce among the isomers. The complex reduces at a potential that is 0.8 V more positive than the free ligand, and 0.4 V more positive than the mono-substituted complex [Pt(3-NO_2-bipy)Cl_2]. We believe this to be due to interaction between the two nitro groups forced by the steric constraints of the 3,3′-substitution (Fig. 1).

Bipy, both in free and coordinated form, tends to undergo two sequential one-electron redox processes. For example, [Pt(bipy)Cl_2] is reduced at −1.06 and −1.79 (Table 1), the separation of 0.7 V being typical of a spin-pairing process of the two electrons in the π* LUMO. We previously reported that [Pt(4,4′-$(NO_2)_2$-bipy)Cl_2] undergoes *four* consecutive one-electron reductions, with the first two being separated by only 0.18 V in DMF solution.[14] We proposed that this was due to a near-degenerate pair of π* orbitals being sequentially singly occupied.

The mono and di-substituted species here also have multiple redox activity. The second reductions of x-NO_2-bipy are 0.8–1.0 V more negative potential than the first, and hence have well separated SLUMOs (second LUMOs). For x,x′-$(NO_2)_2$-bipy the second reductions are only 0.1–0.3 V more negative. For [Pt(x-NO_2-bipy)Cl_2] the gap is 0.4–0.6 V. For [Pt(x,x′-$(NO_2)_2$-bipy)Cl_2] there is a much bigger difference between the two processes for x,x′ = 3 (0.4 V) than for x,x′ = 4 or 5 (0.19 and 0.14 V, respectively), because of the anomalously low first reduction potential.

The electrochemical response of 5,5′-$(NO_2)_2$-bipy (Fig. 2) and [Pt(5,5′-$(NO_2)_2$-bipy)Cl_2] are markedly solvent dependent (Tables S1 and S2, ESI). Systematic studies showed a good correlation (Fig. 3) with the solvent Guttmann acceptor number[35] (a.n.) which is a measure of the solvent Lewis acidity. For example, for 5,5′-$(NO_2)_2$-bipy the two one-electron reductions are observed sequentially in low a.n. solvents (*e.g.* THF, ethyl acetate; Fig. 2a) whereas in solvents with an a.n. of 19 or higher (*e.g.* DMSO, DCM) a single two-electron process is observed (Fig. 2b). Fig. 3 shows that the second reduction potential is effected considerably more than the first; hence it is the interaction of the solvent with

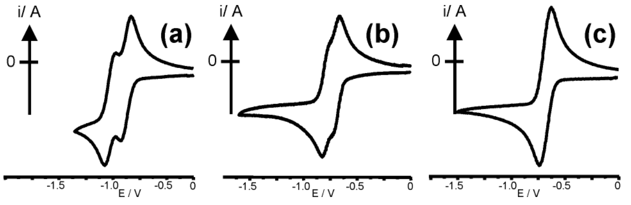

Fig. 2 Cyclic voltammetry of 5,5′-$(NO_2)_2$-bipy *vs.* Ag/AgCl in 0.1 M [$^nBu_4N$][BF_4] solution in (a) THF, (b) DMF and (c) DMSO at 293 K.

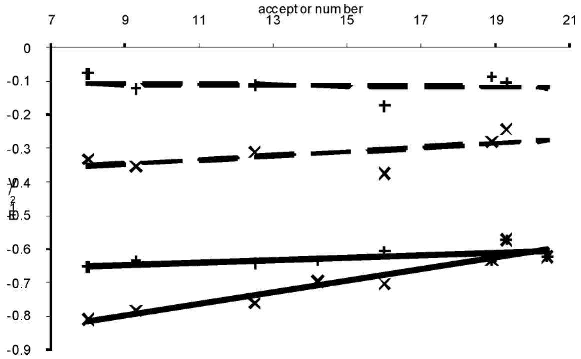

Fig. 3 E_1 (+) and E_2 (×) *vs.* Guttman acceptor number for 5,5′-$(NO_2)_2$-bipy (solid line) and [Pt(5,5′-$(NO_2)_2$-bipy)Cl_2] (dashed).

the dianion that is dominating the effect. The effect is lesser, but still apparent, for [Pt(5,5′-$(NO_2)_2$-bipy)Cl_2] (Fig. 3) reflecting the greater delocalisation of the charge on complexation to {$PtCl_2$}.

UV/Vis/NIR Spectroelectrochemistry

In situ UV/Vis/NIR spectroelectrochemical studies were undertaken for those processes that were reversible on the bulk electrolysis timescale. Full spectroscopic data are given in Table S3,† and we summarise the important points here.

None of the free ligands in their uncharged form have any peaks below 30 kcm^{-1}. On one-electron reduction of x-NO_2-bpy to [x-NO_2-bipy]$^-$, two intense peaks appear at 25–30 and 15–20 kcm^{-1}. This behaviour is similar to that of [x-NO_2-py]$^-$. This implies that the electronic structure is similar, *i.e.* the SOMO is largely localised on the NO_2-bearing ring, also consistent with the redox data (see above). This distinctive pattern is also seen for the disubstituted [4,4′-$(NO_2)_2$-bipy]$^-$, *i.e.* the conjugation between the rings is largely broken. However, the x,x′ = 3 and 5 isomers also have peaks at 8–10 kcm^{-1} which are characteristic of reduced bipyridyls *i.e.* with delocalisation over both rings. These distinct differences in the electronic structures of the [x,x′-$(NO_2)_2$-bipy]$^-$ family are confirmed by EPR (see below).

On complexation of the uncharged ligands to {$PtCl_2$} a metal-to-ligand charge transfer transition is observed at 20–25 kcm^{-1}. The trend in the MLCT energies of [Pt(x,x′-$(NO_2)_2$-bipy)Cl_2] (21.4, 23.0, 22.4 kcm^{-1} for x = 3, 4 and 5, respectively) is consistent with that of the reduction potentials. All the mono-reduced [Pt(x-NO_2-bipy)Cl_2]$^-$ and [Pt(x,x′-$(NO_2)_2$-bipy)Cl_2]$^-$ complexes have the low-energy bands at 7–11 kcm^{-1}, characteristic of reduced bipyridyls. This includes [Pt(4,4′-$(NO_2)_2$-bipy)Cl_2]$^-$ which suggests that there is a pronounced change in the electronic structure of [4,4′-$(NO_2)_2$-bipy]$^-$ on coordination, from localised on a single ring to delocalised over both, presumably related to the forced conformation.

A number of the transitions in the spectra of 5-NO_2-bipy and 5,5′-$(NO_2)_2$-bipy and their complexes showed vibronic structure with spacing of *ca.* 1400 cm^{-1}. This can be attributed to the NO_2 symmetric stretch; IR spectra of 5,5′-$(NO_2)_2$-bipy (KBr disc) show a strong band at *ca.* 1600 cm^{-1}.

EPR Spectroelectrochemistry

The reduction products of the free-ligands and complexes were also studied by *in situ* EPR spectroelectrochemical methods, using the same electrogeneration potentials as in the UV/Vis/NIR experiments. All compounds were EPR silent prior to application of a negative potential, with the exception of [Pt(3,3′-$(NO_2)_2$-bipy)Cl_2] which displayed a weak signal. This is due to its very positive reduction potential (see above). The signal grew in intensity on application of a negative potential, and could be removed entirely at +0.5 V. All resolved hyperfine coupling constants from isotropic (fluid solution) spectra are summarised in Table 2 (including data for x-NO_2-py for comparison). In the discussion below we focus on the ^{14}N and ^{195}Pt coupling.

Table 2 Isotropic *g*-values and hyperfine coupling constants (a/10^{-4} cm^{-1}) and line-widths (ΔH_{pp}/G) from fluid solution EPR spectra

Compound	*g*	ΔH_{pp}	a(^{195}Pt)	a(^{14}N)	a(^{1}H)
[3-NO_2-py]$^-$	2.0048	0.45	—	1 × 8.60 1 × 2.28	1 × 4.29 1 × 3.01 1 × 1.22 1 × 1.14
[4-NO_2-py]$^-$	2.0055	0.30	—	1 × 7.89 1 × 2.27	2 × 2.85 2 × 0.42
[3-NO_2-bipy]$^-$	2.0053	0.60	—	1 × 7.54 1 × 2.20	1 × 4.59 1 × 3.00 1 × 1.21
[4-NO_2-bipy]$^-$	2.0055	0.50	—	1 × 6.74 1 × 2.81	2 × 2.43 1 × 0.38
[5-NO_2-bipy]$^-$	2.0031	1.10	—	1 × 6.64	1 × 3.74 1 × 2.20 1 × 2.29 1 × 1.03
[3,3′-$(NO_2)_2$-bipy]$^-$	2.0037	0.50	—	2 × 3.50	2 × 1.87 2 × 1.29
[4,4′-$(NO_2)_2$-bipy]$^-$	2.0055	0.55	—	1 × 6.34 1 × 2.53	1 × 3.04 1 × 2.80 1 × 0.19
[4,4′-$(^{15}NO_2)_2$-bipy]$^-$	2.0053	0.50	—	1 × 8.89 1 × 2.53	1 × 3.04 1 × 2.80
[5,5′-$(NO_2)_2$-bipy]$^-$	2.0041	0.30	—	2 × 1.54	2 × 1.54 2 × 0.62 2 × 0.35
[Pt(4-NO_2-bipy)Cl_2]$^-$	2.0036	1.40	33.2	1 × 4.21 1 × 3.09	1 × 2.90 1 × 1.40
[Pt(5-NO_2-bipy)Cl_2]$^-$	2.0095	1.00	18.8	—	—
[Pt(3,3′-$(NO_2)_2$-bipy)Cl_2]$^-$	2.0037	1.40	20.1	4 × 1.1	2 × 1.1
[Pt(4,4′-$(NO_2)_2$-bipy)Cl_2]$^-$	2.0018	13.0	37.4	—	—
[Pt(5,5′-$(NO_2)_2$-bipy)Cl_2]$^-$	1.9983	1.00	22.3	—	—

[x-NO_2-bipy]$^-$: for each isomer the dominant hyperfine coupling is to the nitro group ^{14}N nucleus, of magnitude *ca.* 7 × 10^{-4} cm^{-1}. The coupling constants are similar to values observed for [x-NO_2-py]$^-$, supporting their similar electronic structure.

[x,x′-$(NO_2)_2$-bipy]$^-$ (Fig. 4): for x,x′ = 3 and 5, the dominant $\underline{N}O_2$-coupling is now to two equivalent ^{14}N nuclei, with values (3.5 and 1.5 × 10^{-4} cm^{-1}, respectively) reduced by at least a factor of two from those of [x-NO_2-bipy]$^-$. This is consistent with the SOMO now being delocalised over both pyridyl rings. In contrast, for x,x′ = 4 two inequivalent single ^{14}N nulei are observed with couplings 6.3 and 2.5 × 10^{-4} cm^{-1}. Spectra of the isotopically labelled [4,4′-$(^{15}NO_2)_2$-bipy]$^-$ confirm the larger splitting to be to the nitro group and the smaller to a pyridyl-N (Fig. 4c; $a_{(15\,N)}$ = 8.9, $a_{(14\,N)}$ = 2.5 × 10^{-4} cm^{-1}). These coupling constants are similar to those for [4-NO_2-bipy]$^-$.[13] Hence, the SOMO of [4,4′-$(^{15}NO_2)_2$-bipy]$^-$ is largely localised on only one of the nitro-bearing rings, not delocalised over the whole molecule, consistent with the UV/Vis data (see above).

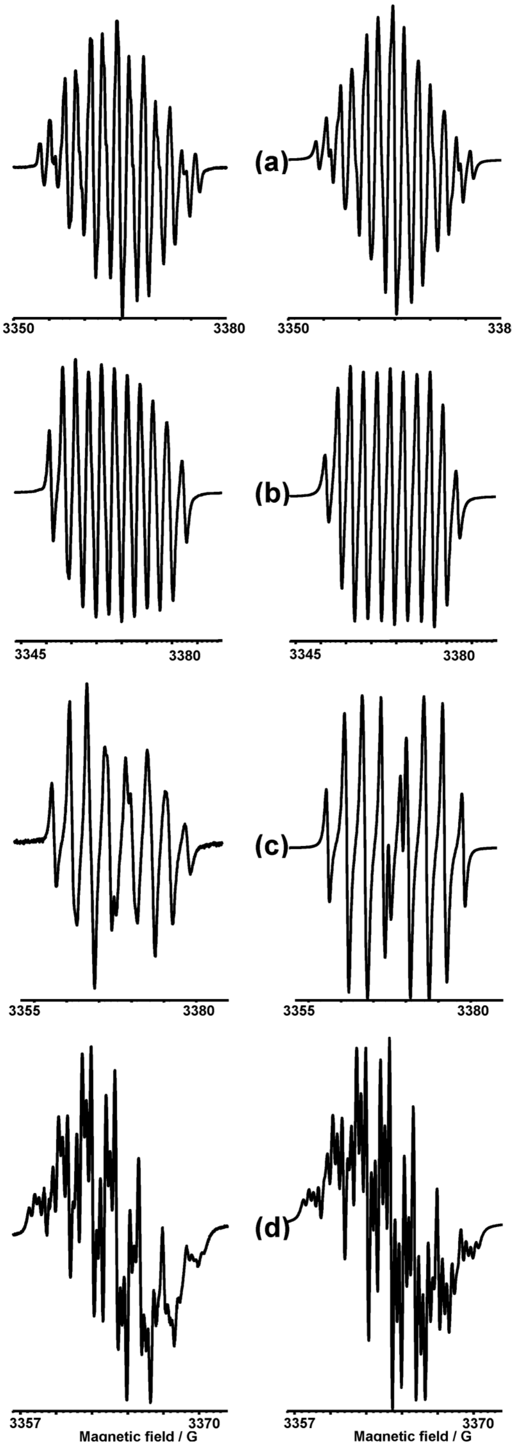

Fig. 4 Experimental (left) and simulated (right) isotropic EPR spectra of (a) $[3,3'\text{-(NO}_2)_2\text{-bipy}]^-$, (b) $[4,4'\text{-(NO}_2)_2\text{-bipy}]^-$, (c) $[4,4'\text{-(}^{15}\text{NO}_2)_2\text{-bipy}]^-$ and (d) $[5,5'\text{-(NO}_2)_2\text{-bipy}]^-$ in 0.1 M $[^n\text{Bu}_4\text{N}][\text{BF}_4]$ DMF at 233 K, generated *in situ* $E_{\text{gen}} = -1.2$ V *vs.* Ag/AgCl.

Mono- and di-reduced forms of $4,4'\text{-(NO}_2)_2$-bipy give identical spectra in fluid solution, differing only in intensity. This implies that the second electron enters an equivalent, and near-degenerate, orbital on the second ring. Formation of a biradical is confirmed by observation of a half-field peak in the frozen solution spectrum (Figure S3†).

The difference in behaviour of $[x,x'\text{-(NO}_2)_2\text{-bipy}]^-$ for x,x′ = 3 or 5 (SOMO delocalised over both rings) and x,x′ = 4 (SOMO largely localised on one ring) may be due to a enhanced preference for a coplanar conformation due to increased conjugation for the former (NO_2 groups *ortho* or *para* to the bridgehead C2 position) *vs.* the latter (NO_2 groups *meta* to C2).

$[Pt(x\text{-}NO_2\text{-}bipy)Cl_2]^-$: For x = 4, coupling is observed to two single ^{14}N (4.2 and 3.1×10^{-4} cm^{-1}), as for the free-ligand radical-anion. We previously showed by ^{15}N labelling that the *smaller* of these couplings is to the nitro-N, in contrast to the free ligand.[13] Hence there is a significant redistribution of the spin density from the nitro group to the pyridyl ring on coordination to a metal ion. In addition, a 33.2×10^{-4} cm^{-1} coupling to ^{195}Pt (33% natural abundance, I = 1/2) is resolved. For x = 5, the only hyperfine structure resolved is to ^{195}Pt: the coupling constant of 19×10^{-4} cm^{-1} is much smaller than for x = 4, showing a much lower spin density at Pt. The x = 3 radical anion proved unstable on the bulk electrosynthesis timescale, even at −40 °C.

$[Pt(x,x'\text{-}(NO_2)_2\text{-}bipy)Cl_2]^-$: ^{195}Pt hyperfine is observed for all three complexes, with values of 20.1, 37.4[14] and 22.3×10^{-4} cm^{-1} for x,x′ = 3, 4 and 5, respectively. Coupling to ligand nuclei is only observed for x,x′ = 3 (1.1×10^{-4} cm^{-1} to four ^{14}N; this is presumably a coincidentally similar coupling to the two nitro and the two ring nitrogens). We previously noted that the x,x′ = 4 isomer has a near-degenerate pair of SOMOs and that there was a huge narrowing of the EPR linewidth from mono- to di-anion;[14] we speculated this to be due to an electron hopping mechanism (between the near degenerate orbitals) in the monoanion which is quenched on occupation of the second orbital. The well resolved spectrum for x,x′ = 3 is then consistent with the much larger separation between the first and second reduction potentials than for x,x′ = 4. The spectrum of the x,x′ = 4 dianion[14] is consistent with delocalisation over both rings.

Frozen solution spectra: On freezing the solutions, well resolved spectra are obtained for all members of the $[\text{Pt}(x,x'\text{-(NO}_2)_2\text{-bipy})\text{Cl}_2]^-$ family (Table 3; Figure S4).[36] We have analysed the ^{195}Pt hyperfine couplings using Maki's equations[37] with Rieger's formalism,[38] as described elsewhere.[11,12] The calculated admixture of Pt valence orbitals (5d and 6p) to the SOMOs are very small (although they dominate the EPR spectra), ranging from 0.5–4%, with the values for x = 4 and 3 the highest and lowest, respectively. These are all significantly smaller than the values derived for the parent, unsubstituted complex $[\text{Pt(bipy)Cl}_2]^-$ (*ca.* 11%),[11,12] obviously due to the electron withdrawing effect of the nitro groups. For the mono-subtituted $[\text{Pt(x-NO}_2\text{-bipy)Cl}_2]^-$ family, only the x = 4 species gives a well resolved spectrum.[13] Similar analysis gives Pt valence orbital admixture to the SOMO of 7%, intermediate between the mono- and un-substituted complexes.

DFT Calculations

DFT calculations were performed on the free ligands and their complexes: selected MO coefficients for the LUMOs are in Table 4. The trends in the electronic structure can be rationalised by considering the LUMO of x-NO_2-py. Unsurprisingly, the LUMO is dominated by the antibonding π* orbital of the nitro group in each case, with a bonding interaction between this fragment and the ring (carbon 2p$_z$). The greatest delocalisation to the ring-N position occurs for x = 4 because only this position allows a

Table 3 Isotropic and anisotropic *g*-values and ^{195}Pt hyperfine coupling constants ($A/10^{-4}$ cm^{-1}) from fluid and frozen solution EPR spectra

	g_{iso}	g_1	g_2	g_3	A_{iso}	A_1	A_2	$A_3{}^a$
$[Pt(4\text{-}NO_2\text{-bipy})Cl_2]^-$	2.005	2.027	2.009	1.985	−33	−29	−53	(−17)
$[Pt(3,3'\text{-}(NO_2)_2\text{-bipy})Cl_2]^-$	2.004	2.015	2.005	1.991	−20	−17	−23	(−20)
$[Pt(4,4'\text{-}(NO_2)_2\text{-bipy})Cl_2]^-$	2.002	2.033	2.006	1.968	−37	−32	−48	(−31)
$[Pt(5,5'\text{-}(NO_2)_2\text{-bipy})Cl_2]^-$	1.998	2.005	2.006	1.963	−22	−19	−29	(−18)

[a] Not resolved experimentally; calculated from $A_{iso} = (A_1 + A_2 + A_3)/3$.

Table 4 Selected DFT calculated % composition of the LUMOs of free ligands and {PtCl$_2$} complexes

Compound	Ring-N 2p$_z$	Nitro-N 2p$_z$	Pt 5d/6p$_z$
$3\text{-}NO_2\text{-py}$	0.9	25.6	—
$4\text{-}NO_2\text{-py}$	10.3	24.7	—
$3\text{-}NO_2\text{-bpy}$	0.6	21.2	—
$4\text{-}NO_2\text{-bpy}$[13]	11.4	23.1	—
$5\text{-}NO_2\text{-bpy}$	1.8	19.3	—
$3,3'\text{-}(NO_2)_2\text{-bpy}$	0.8	11.5	—
$4,4'\text{-}(NO_2)_2\text{-bpy}$	8.2	9.7	—
$5,5'\text{-}(NO_2)_2\text{-bpy}$	3.1	7.7	—
$[Pt(bpy)Cl_2]$[12]	12.9	—	6.6
$[Pt(3\text{-}NO_2\text{-bpy})Cl_2]$	3.4	14.8	2.5
$[Pt(4\text{-}NO_2\text{-bpy})Cl_2]$[13]	16.0	12.4	7.1
$[Pt(5\text{-}NO_2\text{-bpy})Cl_2]$	6.5	8.1	4.2
$[Pt(3,3'\text{-}(NO_2)_2\text{-bpy})Cl_2]$	4.0	7.0	3.0
$[Pt(4,4'\text{-}(NO_2)_2\text{-bpy})Cl_2]$	11.0	4.3	8.8
$[Pt(5,5'\text{-}(NO_2)_2\text{-bpy})Cl_2]$	6.4	3.7	4.4

symmetry match between the nitro group and the the b$_1$ LUMO of pyridine itself (Fig. 5). This argument also holds for all the species in Table 4: the greatest contribution to the LUMO from the ring-N 2p$_z$ orbital is for the x(x′) = 4 isomers. [Note this also explains the trend in reduction potentials for the free ligands, Table 1.] This could also be described in terms of conjugation effects between the nitro group and the ring-N in the 4(4′) substituents (*para*) *vs.* 3(3′) or 5(5′) (both *meta*). This then allows greatest overlap with Pt valence orbitals when coordinated, in agreement with the parameters derived from the EPR data in Table 3. The calculations also support the shift of electron density from nitro-N to ring-N (as observed experimentally from the relative magnitudes of the hyperfine coupling constants) on coordination to the Pt(II) ion.

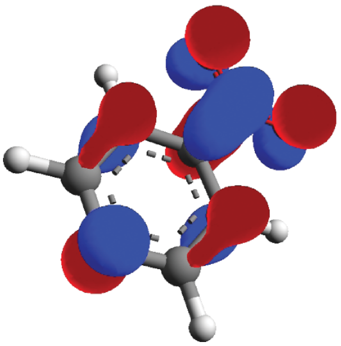

Fig. 5 Calculated LUMO of $4\text{-}NO_2\text{-py}$.

Conclusions

To summarise, we have undertaken a systematic study of the influence of substitution pattern of strongly electron-withdrawing nitro groups on the redox and spectroscopic properties of a series of bipyridines and their complexes with {PtCl$_2$}. We have shown marked differences in the properties of the $x,x'\text{-}(NO_2)_2\text{-bipy}$ family depending on substitution position, including gross changes in the nature of the electron acceptor orbitals. For their complexes there are more subtle variations in the spin distribution, but the reduction potential varies by *ca.* 0.3 V with x,x′. The most remarkable redox behaviour is observed for $[Pt(3,3'\text{-}(NO_2)_2\text{-bipy})Cl_2]$ which reduces at +0.01 V *vs.* Ag/AgCl, whereas $[Pt(3\text{-}NO_2\text{-bipy})Cl_2]$ is the hardest to reduce of the monosubstituted series, which must be partly due to the steric effects of disubstitution at the 3,3′ positions.

Experimental

Synthesis

$3\text{-}NO_2\text{-py}$ was commercially available; $5\text{-}NO_2\text{-bipy}$,[30] and $4,4'\text{-}(NO_2)_2\text{-bipy}$[15] were prepared by literature methods. We have reported $[Pt(4\text{-}NO_2\text{-bipy})Cl_2]$[13] and $[Pt(4,4'\text{-}(NO_2)_2\text{-bipy})Cl_2]$[14] previously.

3-nitro-2,2′-bipyridine ($3\text{-}NO_2\text{-bipy}$): Prepared using the method reported for $5\text{-}NO_2\text{-bipy}$,[30] but with 2-chloro-3-nitropyridine replacing 2-chloro-5-nitropyridine. The beige product precipitated from the solution on filtering through the silica gel/celite bed (yield 70%). Elemental analysis (%), observed (calculated for $C_{10}H_7N_3O_2$): C, 59.25 (59.70), H, 3.53 (3.51), N, 20.55 (20.89). ^{1}H NMR (CD_3Cl, 199.972 MHz): δ = 8.845 (d, *J* = 4.69 Hz, 1H), 8.621 (d, *J* = 4.69 Hz, 1H), 8.621 (d, *J* = 4.69 Hz, 1H), 8.094 (d, *J* = 8.206 Hz, 2H), 7.486 (dd, *J* = 8.20, 4.69 Hz, 1H), 7.384 (dd, *J* = 7.62, 5.02 Hz, 1H) ppm, Mass spectra (EI) *m*/*z*: 201 (M$^+$).

3,3′-dinitro-2,2′-bipyridine ($3,3'\text{-}(NO_2)_2\text{-bipy}$): Adapted from literature preparation.[28] 2-Chloro-3-nitropyridine (5 g, 0.031 mol) was heated to 100 °C with copper bronze (5 g) in DMF (20 ml) for 15 h. The mixture was cooled, diluted with water (70 ml) and filtered. The resulting brown solid was filtered and triturated with ammonia (3 × 4 ml) before being extracted exhaustively with boiling 1,4-dioxane. The brown, crystalline solid obtained was recrystallised with hot filtering from boiling 1,4-dioxane. Yield (1.448 g, 37.9%). Elemental analysis (%), observed (calculated for $C_{10}H_6N_4O_4$): C, 48.89 (48.79), H 2.49 (2.46), N 22.76 (22.76). ^{1}H NMR (CD_3Cl, 199.972 MHz): δ = 8.889 (dd, *J* = 4.69, 1.56 Hz, 2H), 8.594 (dd, *J* = 1.56, 8.20 Hz, 2H), 7.654 (dd, *J* = 8.20, 4.69 Hz, 2H) ppm, Mass spectra (FAB) *m*/*z*: 247 ((M+1)$^+$).

5,5′-dinitro-2,2′-bipyridine ($5,5'\text{-}(NO_2)_2\text{-bipy}$): Adapted from literature preparation.[29] 2-Iodo-5-nitropyridine (14.99 g, 0.059 mol) was dissolved in DMF and treated with copper bronze (50 g). This was stirred and heated to reflux under nitrogen for 7h. The hot mixture was filtered and poured into water (1000 ml). The resulting grey solid was filtered through a sintered funnel, triturated with ammonia solution (3 × 60 ml) and extracted with boiling 1,4-dioxane. After cooling, the 1,4-dioxane extracts were filtered and the resulting solid was recrystallised from 1,4-dioxane. A pale yellow solid was obtained. Further product was obtained by evaporating the filtrate from each 1,4-dioxane extract and recrystallising the resulting solid from 1,4-dioxane. Yield (2.360 g, 16.25%). Elemental analysis (%), observed (calculated for $C_{10}H_6N_2O_2$): C, 48.42 (48.79), H 2.42 (2.46), N 22.43 (22.76). ^{1}H NMR (CD_3Cl, 199.972 MHz): $\delta = 9.546$ (d, $J = 2.34$ Hz, 2H), 8.786 (d, $J = 8.59$ Hz, 2H), 8.667 (dd, $J = 8.52, 2.74$ Hz, 2H) ppm, Mass spectra (EI) m/z: 246 (M^+).

Pt Complexes: The ligand was suspended in water and heated to reflux with a molar equivalent of $K_2[PtCl_4]$ and the precipitated product was filtered off. [Pt(5,5′-$(NO_2)_2$-bipy)Cl_2] was recrystallised from DMSO whereas [Pt(3,3′-$(NO_2)_2$-bipy)Cl_2] was dissolved in DMF and precipitated slowly by diffusion of Et_2O. For complexes of 5,5′-$(NO_2)_2$-bpy the solutions required heating for 48 h to obtain a reasonable yield; for the other ligands heating was for 24 h.

[Pt(3-NO_2-bipy)Cl_2]: Orange solid (96%). Elemental analysis (%), observed (calculated for $C_{10}H_7N_3O_2PtCl_2$): C, 26.62 (25.71), H 1.53 (1.51), N 8.66 (8.99).

[Pt(3,3′-$(NO_2)_2$-bipy)Cl_2]: Dark red crystalline solid (85%). Elemental analysis (%), observed (calculated for $C_{10}H_6N_4O_4PtCl_2$): C, 23.27 (23.45), H 1.53 (1.18), N 10.53 (10.94).

[Pt(4,4′-$(NO_2)_2$-bipy)Cl_2]:[14] Dark green crystalline solid (60%). Elemental analysis (%), observed (calculated for $C_{10}H_6N_4O_4PtCl_2$): C, 23.04 (23.45), H 0.91 (1.18), N 10.35 (10.94).

[Pt(5-NO_2-bipy)Cl_2]: Dark red/brown solid (86%). Elemental analysis (%), observed (calculated for $C_{10}H_7N_3O_2PtCl_2$): C, 31.77 (25.71), H 2.10 (1.51), N 9.57 (8.99).

[Pt(5,5′-$(NO_2)_2$-bipy)Cl_2]: Brown solid (71%). Elemental analysis (%), observed (calculated for $C_{10}H_6N_4O_4PtCl_2$): C, 24.04 (23.45), H 1.46 (1.18), N 10.04 (10.94).

Crystallography

3-NO_2-bipy. $C_{10}H_7N_3O_2$, $M = 201.19$, orthorhombic, $a = 7.4647(3)$, $b = 10.1931(4)$, $c = 11.7396(4)$ Å, $U = 893.25(6)$ Å^3, $T = 150$ K, space group $P2_12_12_1$, $Z = 4$, 5306 reflections measured, $R_{int} = 0.0447$. Final wR_2 [$I > 2\sigma(I)$] = 0.0674.

5,5′-$(NO_2)_2$-bipy.dioxane. Pale yellow block grown from dioxane, $C_{14}H_{14}N_4O_6$, $M = 334.29$, triclinic, $a = 6.4941(6)$, $b = 6.5761(6)$, $c = 9.3664(8)$ Å, $\alpha = 85.200(1)$, $\beta = 87.910(1)$, $\gamma = 66.005(1)°$, $U = 364.15(6)$ Å^3, $T = 150$ K, space group $P\bar{1}$, $Z = 4$, 3240 reflections measured, $R_{int} = 0.0135$. Final wR_2 [$I > 2\sigma(I)$] = 0.1175.

2[Pt(3,3′-$(NO_2)_2$-bipy)Cl_2].dmf. Dark red crystals grown from diffusion of Et_2O into DMF solution. $C_{23}H_{19}Cl_4N_9O_9Pt_2$, $M = 1097,45$, triclinic, $a = 14.3359(12)$, $b = 14.1844(13)$, $c = 14.9479(13)$ Å, $\beta = 99.909(2)°$, $U = 2994.3(4)$ Å^3, $T = 150$ K, space group $P2_1/n$, $Z = 4$, 7311 reflections measured, $R_{int} = 0.0311$. Final wR_2 [$I > 2\sigma(I)$] = 0.0604.

Analysis

Electrochemical studies used an Autolab PGSTAT30 potentiostat with General Purpose Electrochemistry system (GPES v 4.8) software. A 3-electrode system was used with Pt microworking, Pt rod counter and Ag/AgCl reference electrodes. All electrochemical studies were carried out in N_2 purged 0.1 M [^{n}Bu$_4$N][BF$_4$] DMF solutions. Data quoted were recorded at 0.1 V s^{-1} scan rate. All values quoted are referenced to Ag/AgCl, against which the ferrocinium/ferrocene couple is measured at +0.55 V. Bulk electrolysis was carried out in an H-cell with a Pt basket working electrode. Electro-generations were carried out at –40 °C (dry ice/acetone bath) under a nitrogen atmosphere.

In situ UV/Vis/NIR electro-generation was performed using an optically transparent thin layer electrode (OTTLE) cell[39] in a Perkin-Elmer Lambda 9 spectrophotometer, with spectra recorded every ten minutes. The potential was set back to. Reversibility was tested by re-generation of the original species.

X-band EPR data were recorded on a Bruker ER 200-D SRC spectrometer connected to a datalink 486DX desktop PC running EPR Acquisition System version 2.42. A variable temperature *in situ* electrolysis cell was used, as described elsewhere.[40] Simulations used Bruker WINEPR Simfonia Version 1.25; g-values were calibrated against 2,2′-diphenyl-1-picrylhydrazyl (DPPH).

DFT calculations used Gaussian 03 (revision D.01).[41] The images were generated using Arguslab.[42] The EPRIII basis set was used for the C, N, H, O, the 6-31G* basis set for the Cl atoms VDZ (n + 1) ECP basis sets for the Pt(II) centre.[43]

Acknowledgements

We acknowledge Professor Peter Tasker for many useful discussions on the subject of resonance structures and congratulate him on his 65th birthday and retirement. We are grateful to the EPSRC for funding the National EPR Facility.

Notes and references

1 G. Ajayakumar, K. Sreenath and K. R. Gopidas, *Dalton Trans.*, 2009, 1180–1186.
2 R. Carmieli, Q. Mi, A. B. Ricks, E. M. Giacobbe, S. M. Mickley and M. R. Wasielewski, *J. Am. Chem. Soc.*, 2009, **131**, 8372–8373.
3 A. Schunter, J. Huo, J. Hoberg and B. P. Sullivan, *Abstracts, 20th Rocky Mountain Regional Meeting of the American Chemical Society, Denver, CO, United States, August 29-September 1 FIELD Full Journal Title:Abstracts, 20th Rocky Mountain Regional Meeting of the American Chemical Society, Denver, CO, United States, August 29-September 1*, 2007, RM-012.
4 E. A. M. Geary, N. Hirata, J. Clifford, J. R. Durrant, S. Parsons, A. Dawson, L. J. Yellowlees and N. Robertson, *J. Chem. Soc. Dalton Trans.*, 2003, 3757–3762.
5 E. A. M. Geary, K. L. McCall, A. Turner, P. R. Murray, E. J. L. McInnes, L. A. Jack, L. J. Yellowlees and N. Robertson, *J. Chem. Soc. Dalton Trans.*, 2008, 3701–3708.
6 E. A. M. Geary, L. J. Yellowlees, L. A. Jack, I. D. H. Oswald, S. Parsons, N. Hirata, J. R. Durrant and N. Robertson, *Inorg. Chem.*, 2005, **44**, 242–250.
7 L. P. Moorcraft, A. Morandeira, J. R. Durrant, J. R. Jennings, L. M. Peter, S. Parsons, A. Turner, L. J. Yellowlees and N. Robertson, *Dalton Trans.*, 2008, 6940–6947.
8 P. V. Bernhardt, G. K. Boschloo, F. Bozoglian, A. Hagfeldt, M. Martinez and B. Sienra, *New J. Chem.*, 2008, **32**, 705–711.
9 G. Kreisel, S. Meyer, D. Tietze, T. Fidler, R. Gorges, A. Kirsch, B. Schäfer and S. Rau, *Chem. Ing. Tech.*, 2007, **79**, 153–159.
10 D. Collison, F. E. Mabbs, E. J. L. McInnes, K. J. Taylor, A. J. Welch and L. J. Yellowlees, *J. Chem. Soc., Dalton Trans.*, 1996, 329–334.
11 E. J. L. McInnes, R. D. Farley, S. A. Macgregor, K. J. Taylor, L. J. Yellowlees and C. C. Rowlands, *J. Chem. Soc., Faraday Trans.*, 1998, **94**, 2985–2991.
12 E. J. L. McInnes, R. D. Farley, C. C. Rowlands, A. J. Welch, L. Rovatti and L. J. Yellowlees, *J. Chem. Soc., Dalton Trans.*, 1999, 4203–4208.

13 P. Murray, L. Jack, E. J. L. McInnes and L. J. Yellowlees, *Dalton Trans.*, 2010, **39**, 4179–4185.

14 E. J. L. McInnes, A. J. Welch and L. J. Yellowlees, *Chem. Commun.*, 1996, 2393.

15 D. Wenkert and R. B. Woodward, *J. Org. Chem.*, 1983, **48**, 283–289.

16 Jones, *J. Chem. Soc. B*, 1967, 84–85.

17 J. Skarzewski and J. Mlochowski, *Heterocycles*, 1979, **12**, 1403–1406.

18 M. J. Cook, A. P. Lewis, G. S. G. McAuliffe, V. Skarda, A. J. Thomson, J. L. Glasper and D. J. Robbins, *J. Chem. Soc. Dalton Trans.*, 1984, 1293–1301.

19 A. B. P. Lever, *Inorg. Chem.*, 1990, **29**, 1271–1285.

20 H. S. K. W. Roland Krassnig, *Helv. Chim. Acta*, 2000, **83**, 380–383.

21 Z. Zhou, G. H. Sarova, S. Zhang, Z. Ou, F. T. Tat, K. M. Kadish, L. Echegoyen, D. M. Guldi, D. I. Schuster and S. R. Wilson, *Chem.–Eur. J.*, 2006, **12**, 4241–4248.

22 J. Otsuki, A. Imai, K. Sato, D.-M. Li, M. Hosoda, M. Owa, T. Akasaka, I. Yoshikawa, K. Araki, T. Suenobu and S. Fukuzumi, *Chem.–Eur. J.*, 2008, **14**, 2709–2718.

23 A. Basu, H. D. Gafney and T. C. Strekas, *Inorg. Chem.*, 1982, **21**, 2231–2235.

24 A. Basu, M. A. Weiner, T. C. Strekas and H. D. Gafney, *Inorg. Chem.*, 1982, **21**, 1085–1092.

25 H.-W. Tseng, R. Zong, J. T. Muckerman and R. Thummel, *Inorg. Chem.*, 2008, **47**, 11763–11773.

26 T. Kikuchi, J. Takagi, T. Ishiyama and N. Miyaura, *Chem. Lett.*, 2008, **37**, 664–665.

27 F. Hildebrand, C. Kohlmann, A. Franz and S. Lütz, *Adv. Synth. Catal.*, 2008, **350**, 909–918.

28 S. Kanoktanaporn and J. A. H. MacBride, *J. Chem. Soc., Perkin Trans. 1*, 1978, 1126–1131.

29 F. Calogero, H. S. Freeman, J. F. Esancy, W. M. Whaley and B. J. Dabney, *Dyes Pigm.*, 1987, **8**, 431–447.

30 B. Zhang and R. Breslow, *J. Am. Chem. Soc.*, 1997, **119**, 1676–1681.

31 M. Pilkington, S. Capelli, J. Hauser, C. Hoffmann and H. B. Burgi, *Acta Crystallogr., Sect. C: Cryst. Struct. Commun.*, 1997, **53**, 1719–1721.

32 C. R. Rice, J. D. Wallis and D. C. Povey, *Acta Crystallogr., Sect. C: Cryst. Struct. Commun.*, 1992, **48**, 1988–1991.

33 V. M. Miskowski, V. H. Houlding, C. M. Che and Y. Wang, *Inorg. Chem.*, 1993, **32**, 2518–2524.

34 J. Yoo, J.-H. Kim, Y. S. Sohn and Y. Do, *Inorg. Chim. Acta*, 1997, **263**, 53–60.

35 V. Gutmann, *The Donor–Acceptor Approach to Molecular Interactions*, Plenum Press, New York, 1978.

36 We have recently studied the x,x′ = 3 compound by *in situ* Q- and W-band EPR spectroelectrochemistry; P. R. Murray, D. Collison, S. Daff, R. Edge, B. W. Flynn, L. Jack, F. Leroux, E. J. L. McInnes, A. F. Murray, D. Sells, T. Stevenson, J. Wolowska and L. J. Yellowlees, *J. Magn. Reson.*, DOI: 10.1016/j.jmr.2011.09.041.

37 A. H. Maki, N. Edelstein, A. Davison and R. H. Holm, *J. Am. Chem. Soc.*, 1964, **86**, 4580–4587.

38 P. H. Rieger, *J. Magn. Reson.*, 1997, **124**, 140–146.

39 S. A. Macgregor, E. McInnes, R. J. Sorbie and L. J. Yellowlees, Spectroelectrochemical (UV/Vis/near IR, EPR) studies of coordination complexes, in *Molecular Electrochemistry of Inorganic Bioinorganic and Organometallic Compounds*, ed. A. J. L. Pombeiro and J. A. McCleverty, Kluwer, Dordrecht, 1993, 503.

40 P. Murray and L. Yellowlees, in *Spectroelectrochemistry*, ed. W. Kaim and A. Klein, Royal Society of Chemistry, Cambridge, 2008.

41 M. J. Frisch , G. W. Trucks, H. B. Schlegel, G. E. Scuseria, M. A. Robb, J. R. Cheeseman, J. A. Montgomery, Jr., T. Vreven, K. N. Kudin, J. C. Burant, J. M. Millam, S. S. Iyengar, J. Tomasi, V. Barone, B. Mennucci, M. Cossi, G. Scalmani, N. Rega, G. A. Petersson, H. Nakatsuji, M. Hada, M. Ehara, K. Toyota, R. Fukuda, J. Hasegawa, M. Ishida, T. Nakajima, Y. Honda, O. Kitao, H. Nakai, M. Klene, X. Li, J. E. Knox, H. P. Hratchian, J. B. Cross, V. Bakken, C. Adamo, J. Jaramillo, R. Gomperts, R. E. Stratmann, O. Yazyev, A. J. Austin, R. Cammi, C. Pomelli, J. Ochterski, P. Y. Ayala, K. Morokuma, G. A. Voth, P. Salvador, J. J. Dannenberg, V. G. Zakrzewski, S. Dapprich, A. D. Daniels, M. C. Strain, O. Farkas, D. K. Malick, A. D. Rabuck, K. Raghavachari, J. B. Foresman, J. V. Ortiz, Q. Cui, A. G. Baboul, S. Clifford, J. Cioslowski, B. B. Stefanov, G. Liu, A. Liashenko, P. Piskorz, I. Komaromi, R. L. Martin, D. J. Fox, T. Keith, M. A. Al-Laham, C. Y. Peng, A. Nanayakkara, M. Challacombe, P. M. W. Gill, B. G. Johnson, W. Chen, M. W. Wong, C. Gonzalez and J. A. Pople, *GAUSSIAN 03 (Revision D.01)*, Gaussian, Inc., Wallingford, CT, 2004.

42 M. A. Thompson, Seattle, WA, Planaria Software LLC, Editon edn.

43 P. J. Hay and W. R. Wadt, *J. Chem. Phys.*, 1985, **82**, 299–310.